

## New semiquantitative assessment of $^{123}\text{I}$ -FP-CIT by an anatomical standardization method

Seiko TAKADA,\* Mana YOSHIMURA,\* Hiroaki SHINDO,\* Kazuhiro SAITO,\*  
Kiyoshi KOIZUMI,\* Hiroya UTSUMI\*\* and Kimihiko ABE\*

\*Department of Radiology and \*\*Third Department of Internal Medicine, Tokyo Medical University

We evaluated a new semiquantitative procedure to more easily and objectively estimate the striatal uptake of  $^{123}\text{I}$ -FP-CIT in patients with Parkinsonian syndrome (PS) and essential tremor (ET), using an anatomical standardization method, the Neurostat. **Methods:** Eleven patients with PS and 8 with ET were examined by clinical assessment and  $^{123}\text{I}$ -FP-CIT SPECT imaging. The modified Hoehn and Yahr Staging Scale and Unified Parkinson's Disease Rating Scale (UPDRS) were used to assess the stage and severity of the disease. The co-registered MR and SPECT images were created with fusion software included in Neurostat. On the cross section, which shows the largest area of striate, irregular shaped regions of interest corresponding to the striate and occipital cortex were drawn. Then the ratio of specific striatal uptake to non-specific occipital cortex,  $V3''(\text{F})$ , was calculated. Another calculation was done by VOIClassic, which is a software included in Neurostat to estimate the counts per voxel of anatomically defined regions such as caudate nucleus, putamen, occipital cortex, and total cortex. Using these count data, the ratio of specific striatal uptake to non-specific occipital cortex,  $V3''(\text{OC})$ , and total cortex,  $V3''(\text{TC})$ , was calculated. **Results:** A fair linear correlation was observed between  $V3''(\text{OC})$  and  $V3''(\text{F})$  ( $y = 1.53x + 1.40$ ;  $r = 0.756$ ;  $p < 0.01$ ), as well as between  $V3''(\text{TC})$  and  $V3''(\text{F})$  ( $y = 1.24x + 1.43$ ;  $r = 0.713$ ;  $p < 0.01$ ). Both  $V3''(\text{OC})$  and  $V3''(\text{TC})$  yielded similar tendencies. Concerning discrimination between ET and PS, there was a significant difference between the mean  $V3''$  of PS and ET ( $p < 0.01$ ). Concerning the correlation between  $V3''$  value and the severity of PS, the UPDRS motor score significantly correlated with the  $V3''(\text{F})$  value ( $r_s = -0.816$ ). However,  $V3''(\text{OC})$  and  $V3''(\text{TC})$  correlated less with UPDRS ( $r_s = -0.667$  and  $-0.645$ , respectively). **Conclusions:** Semiquantitative parameters,  $V3''(\text{OC})$  and  $V3''(\text{TC})$ , calculated by VOIClassic including the Neurostat system are useful and easily calculable parameters as well as  $V3''(\text{F})$  for the differential diagnosis of PS from ET.

**Key words:**  $^{123}\text{I}$ -FP-CIT, Parkinson's disease, dopamine transporters, single-photon emission computed tomography, anatomical standardization

### INTRODUCTION

PARKINSON'S DISEASE (PD) is characterized by an insidious onset with slowing of voluntary movement, muscular rigidity, postural abnormality and tremors. The condition of the disease progresses in the first 4 years more rapidly than in later phases, and so rapid and accurate diagnosis in

the early stage is important for successful treatment. Since the most common presenting symptoms include tremor, distinguishing PD-related tremor from essential tremor (ET) is important yet clinically difficult because of the overlapping of the tremor frequency in some atypical cases. Moreover there are no distinctive features to differentiate them by diagnostic imaging such as CT, MRI and scintigraphy. Despite the known benefit of levodopa in reducing the symptoms of PD, it is not desirable to use levodopa for diagnostic purposes or for treatment in the early stage because it might hasten neurodegeneration and at least 50% of patients with PD develop complications within the first 5 years of treatment with levodopa.

Received December 5, 2005, revision accepted June 14, 2006.

For reprint contact: Seiko Takada, M.D., Department of Radiology, Tokyo Medical University, 6-7-1 Nishi-Shinjuku, Shinjuku-ku, Tokyo 160-0023, JAPAN.

*N*-(3-fluoropropyl)-2 $\beta$ -carbomethoxy-3 $\beta$ -(4-iodophenyl)nortropane ( $^{123}\text{I}$ ) ( $^{123}\text{I}$ -FP-CIT)<sup>1-4</sup> is a cocaine analog with high affinity for dopamine transporters (DATs). The presence of DATs can be exploited to image the nigrostriatal neuron viability/density. In patients with Parkinsonian syndrome (PS) the reduction of DAT binding occurs in the putamen and caudate nucleus although no involvement occurs in patients with ET.  $^{123}\text{I}$ -FP-CIT provides an additional tool to help the clinician confirm the diagnosis of PS.

As for the semiquantitative analysis, a receptor parameter,  $V_3''$ , is reported to represent the specific-to-nonspecific equilibrium partition coefficient defined as the equilibrium volume of distribution of the specific compartment relative to that of the nonspecific binding.<sup>5</sup> The  $V_3''$  value in this study represents striatal uptake of the tracer relative to nonspecific uptake to some cerebral cortex to evaluate the capacity of DATs in patients with Parkinsonian syndrome. However several methods are used for measurement of striatal uptake, e.g., to set oval regions of interest (ROIs) on anywhere in bilateral striatal regions with optional size,<sup>6,7</sup> or to make irregularly shaped ROIs by means of fusion imaging with either MRI or CT.<sup>8,9</sup> On the other hand, ROIs, which represent the uptake of the non-specific region, are sometimes selected in the occipital lobe, frontal lobe<sup>6,7</sup> or cerebellum.<sup>6,8</sup> To apply oval ROIs is a simple and easy procedure, but it can be arbitrary, especially when the uptake is faint. To perform fusion imaging and trace the striatal region on the images might be more correct and objective, but other imaging data such as CT or MRI are needed. We therefore tried a new semiquantitative procedure to more easily and objectively estimate the uptake of striatal regions of  $^{123}\text{I}$ -FP-CIT in patients with PS and ET by using an anatomical standardization method, the Neurostat. It was developed by Minoshima et al.<sup>10</sup> for the objective interpretation of functional brain images and validated as effective as the statistical parametric mapping (SPM) in FDG-PET images of normal brain.<sup>11</sup> But its effectiveness is established only for the analysis of pharmaceuticals which distribute to the whole brain. So we investigated if it is also useful in the case of localized distribution such as  $^{123}\text{I}$ -FP-CIT. For clinical evaluation, we compared the feasibility of distinguishing between PS and ET by Neurostat with the fusion method as a gold standard, and moreover, in cases of PD, sought to determine if there is a correlation between the semiquantitative estimation of striatal uptake of the radioligand and clinical features.

## MATERIALS AND METHODS

### Patients

Eleven patients with PS (4 men and 7 women, age 40–78,  $61.9 \pm 9.9$ ), including 9 with PD, one progressive supranuclear palsy (PSA), and one multiple system atrophy (MSA), and 8 ET patients (4 men and 4 women, age 50–

79,  $67.8 \pm 9.6$ ) were examined by clinical assessment and  $^{123}\text{I}$ -FP-CIT SPECT imaging. ET patients are diagnosed based on the presence of postural tremor without resting tremor, rigidity, akinesia, and disturbance of retaining posture, and whose symptoms are ameliorated by  $\beta$  blocker. The modified Hoehn and Yahr Staging Scale and Unified Parkinson's Disease Rating Scale (UPDRS) were used to assess the stage and severity of the disease. The number of patients categorized according to the modified Hoehn and Yahr Staging Scale was 2 as PD1, 1 as PD2, 1 as PD2.5, 2 as PD3, and 3 as PD4. The scale of both 1 patient with PSA and 1 with MSA was 4. All subjects signed a written informed consent form according to the study protocol approved by the ethics committee of Tokyo Medical University.

### Image acquisition

The tracer, 167 MBq of  $^{123}\text{I}$ -FP-CIT was supplied by Nihon Medi-Physics Co. Ltd. (Tokyo, Japan). We performed  $^{123}\text{I}$ -FP-CIT imaging 3, 4 and 6 hours after intravenous injection.

SPECT imaging was performed using a triple-headed SPECT system (Prism 3000XP, Picker International, Inc., Cleveland, OH) equipped with ultra-high resolution fan beam collimators and interfaced with a dedicated computer (Odyssey VP; Picker International, Inc., Cleveland, OH). Images were acquired by 120 degrees rotation (3 degrees per step, total acquisition time of 20 minutes) on a  $128 \times 128$  matrix with a 10% symmetrical window centered at 159 keV and reconstructed by filtered backprojection with a Butterworth filter (order of 8.0 and cut-off of 0.26). Attenuation correction was done by the Chang method (attenuation coefficient of 0.09). Slice thickness finally displayed was 10.5 mm. For the analysis, 4-hour images were used because their image quality was better with regard to background clearance and total acquisition counts.

### Data analysis

#### 1) Manual ROI method in fused MR images

The MRI study was used to remap individual anatomy in each SPECT study. MRI was performed using a 1.5T imaging system (Symphony, Siemens Medical Solutions, Germany) and 0.5T imaging system (MAGNEX 150, Shimadzu Medical Systems, Kyoto, Japan) with a head coil. MR pulse sequences consisted of axial spin-echo T1-weighted image and T2-weighted image without interslice gap. The co-registered MR and SPECT images were created with a fusion software based on the mutual information principle included in Neurostat. Then on the cross section, which shows the largest area of striate, irregular shaped ROIs corresponded to the striate (both the head of the caudate nucleus and putamen) as the specific uptake, and the occipital cortex as the non-specific uptake (Fig. 1). Then the ratio of specific to non-specific uptake, called  $V_3''(F)$ , was calculated by the following formula. The

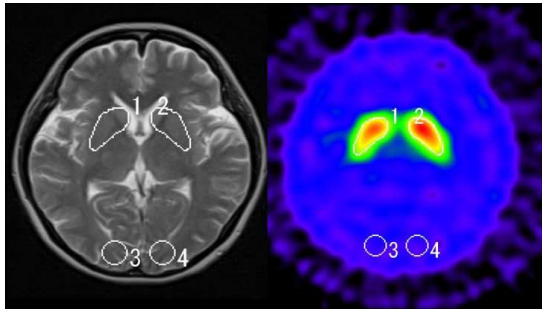


**Fig. 1** Irregular shaped ROIs were drawn on the striatum and the occipital cortex on the fused MRI.

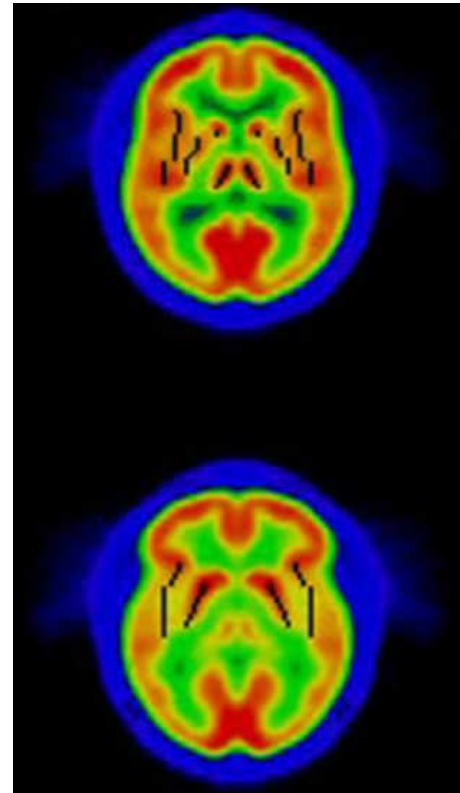
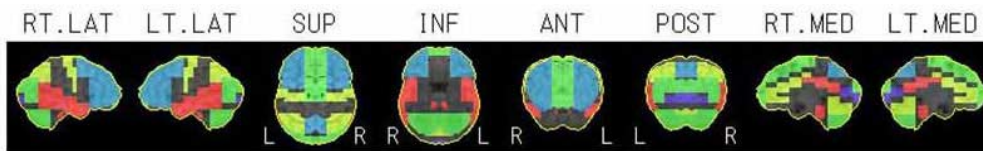


**Fig. 2** The reference regions on the FDG template for the caudate nucleus, putamen, thalamus, and parahippocampus gyrus are shown.

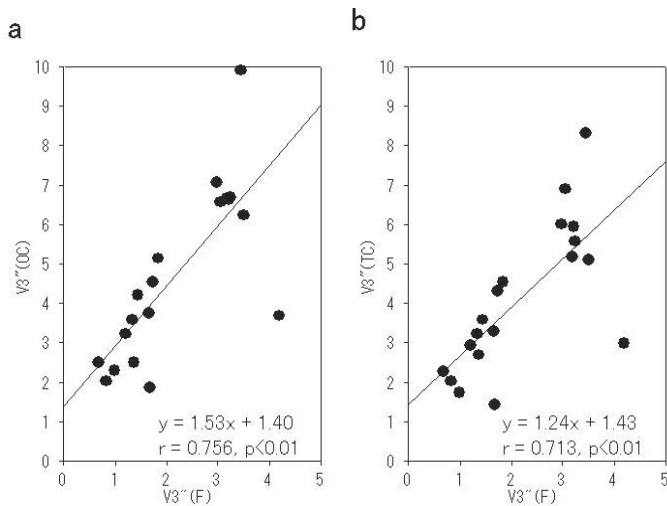


		ave	area
Parietal Association Cortex	Lt	463.479034	286
	Rt	467.713287	286
Temporal Association Cortex	Lt	466.466064	648
	Rt	489.091064	648
Frontal Association Cortex	Lt	459.097778	1074
	Rt	473.829620	1074
Occipital Association Cortex	Lt	439.088898	405
	Rt	454.985199	405
Posterior Cingulate Cortex	Lt	431.320648	184
	Rt	426.369568	184
Anterior Cingulate Cortex	Lt	732.881775	313
	Rt	705.175720	313
Medial Frontal Cortex	Lt	463.903412	818
	Rt	453.902191	818
Medial Parietal Cortex	Lt	489.257294	206
	Rt	474.417480	206
Primary Sensorimotor Cortex	Lt	513.162292	191
	Rt	488.523804	189
Primary Visual Cortex	Lt	424.551208	205
	Rt	377.702454	205

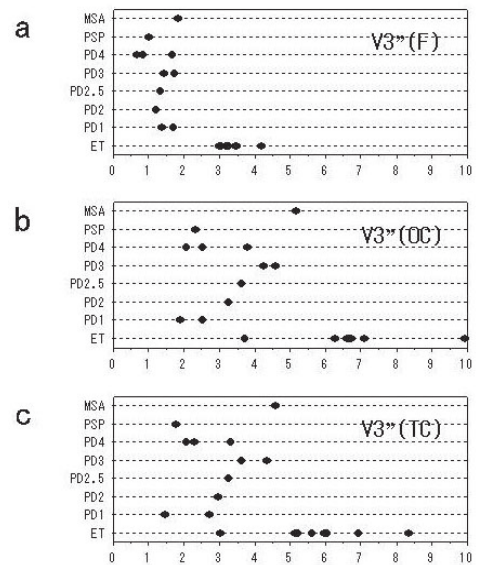
  

		ave	area
Caudate Nucleus	Lt	2052.666748	15
	Rt	1930.933350	15
Cerebellar Hemisphere	Lt	453.257294	618
	Rt	459.846283	618
Cerebellar Vermis	Lt	454.891388	221
	Rt	465.746613	221
Pons		573.893311	300
Putamen	Lt	1412.681274	91
	Rt	1450.604370	91
Parahippocampus Gyrus	Lt	534.357117	56
	Rt	618.482117	56
Amygdala	Lt	489.625000	16
	Rt	515.875000	16
Thalamus	Lt	529.628601	35
	Rt	605.200012	35
Averaged Cerebral Cortex		492.531952	9324
Averaged Global Activity		501.624329	15964

**Fig. 3** VOIClassic Data sheet. Every area in VOIClassic consists of several voxels, and each voxel means a 2.25 mm × 2.25 mm × 2.25 mm cube. The average count of each voxel in the corresponding area is calculated. This sheet is of an ET patient whose SPECT image is shown in Figure 7. Average count of caudate nucleus is Lt: 2053, Rt: 1931. Putamen is Lt: 1413, Rt: 1451. Occipital association cortex is Lt: 439, Rt: 455, and averaged cerebral cortex is 493.



**Fig. 4**  $V3''(OC)$  and  $V3''(TC)$  values were plotted against  $V3''(F)$ . Good linear correlation was observed between  $V3''(OC)$  or  $V3''(TC)$  and  $V3''(F)$ .



**Fig. 5**  $V3''$  values for each of the diseases are plotted. Though  $V3''(F)$  showed the markedly lower values, the distribution patterns were similar.

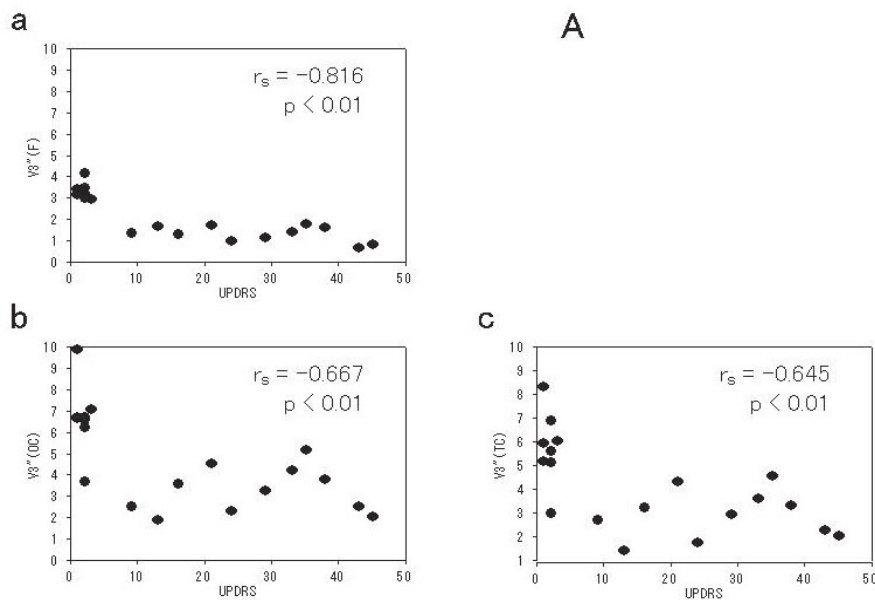


**Fig. 6**  $V3''$  values are plotted against the UPDRS motor score.  $V3''(F)$  value was significantly correlated with UPDRS motor score.

mean values of the right and left regions were used for the calculation.

$V3''(F) = (\text{striate counts per pixel} - \text{occipital cortex counts per pixel}) / \text{occipital cortex counts per pixel}$

## 2) Automatic ROI method by anatomical standardization

VOIClassic is a software included in Neurostat to automatically calculate the counts of anatomically defined regions in the brain. It uses stereotactic anatomic standardization, which confirms the line between the anterior and posterior commissure from the SPECT/PET

**Table 1** Comparison of V3'' values in the disease groups

Diagnosis	Patient number	V3''(F)	V3''(OC)	V3''(TC)
Essential tremor	8	3.34 ± 0.38	6.71 ± 1.67	5.78 ± 1.53
Parkinson syndrome	11	1.33 ± 0.38	3.27 ± 1.10	2.93 ± 1.01
Significance		< 0.01	< 0.01	< 0.01

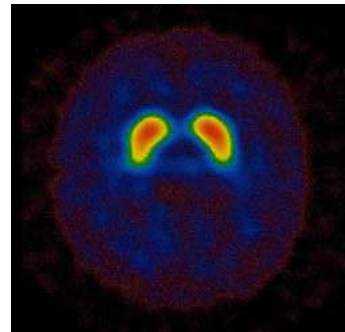


**Fig. 7** An ET patient: SPECT image. High activity in the basal ganglia is shown.

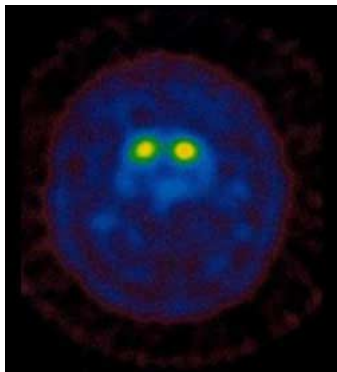
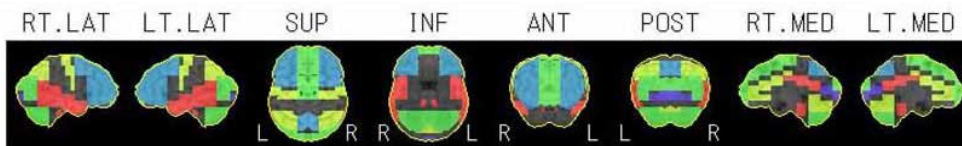


**Fig. 8** A PD patient with modified Hoehn and Yahr Staging Scale of 2: (a) SPECT image. Activity in the basal ganglia is faint. (b) VOIClassic Data sheet. Average count of caudate nucleus is Lt: 1246, Rt: 1181. Putamen is Lt: 540, Rt: 618. Occipital association cortex is Lt: 419, Rt: 422, and averaged cerebral cortex is 456.

a



		ave	area
Parietal Association Cortex	Lt	399.125885	286
	Rt	412.636353	286
Temporal Association Cortex	Lt	470.327148	648
	Rt	451.966064	648
Frontal Association Cortex	Lt	468.870575	1074
	Rt	446.556793	1074
Occipital Association Cortex	Lt	418.530853	405
	Rt	421.918518	405
Posterior Cingulate Cortex	Lt	465.961945	184
	Rt	485.902161	184
Anterior Cingulate Cortex	Lt	583.217224	313
	Rt	603.507996	313
Medial Frontal Cortex	Lt	457.032043	780
	Rt	454.468597	796
Medial Parietal Cortex	Lt	438.067963	206
	Rt	416.524261	206
Primary Sensorimotor Cortex	Lt	427.433533	173
	Rt	417.942200	173
Primary Visual Cortex	Lt	410.463409	205
	Rt	411.951233	205

		ave	area
Caudate Nucleus	Lt	1246.066650	15
	Rt	1181.266724	15
Cerebellar Hemisphere	Lt	588.066345	618
	Rt	573.545288	618
Cerebellar Vermis	Lt	402.873291	221
	Rt	391.660645	221
Pons	Lt	491.253326	300
	Rt		
Putamen	Lt	539.560425	91
	Rt	618.439575	91
Parahippocampus Gyrus	Lt	418.714294	56
	Rt	480.357147	56
Amygdala	Lt	400.562500	16
	Rt	468.625000	16
Thalamus	Lt	704.742859	35
	Rt	587.571411	35
Averaged Cerebral Cortex		456.021118	9230
Averaged Global Activity		470.187317	15904

b

data and matches the individual images to the template of the Talairach atlas using an automated linear and nonlinear warping. The reference region on the FDG template for the caudate nucleus and the putamen is shown (Fig. 2). Every area in VOIClassic (Fig. 3) consists of several voxels and each voxel means a 2.25 mm × 2.25 mm × 2.25 mm cube. The average count of each voxel including the caudate nucleus and the putamen divided by the atlas grid was analyzed. The specific uptake to the striate was calculated by the summation of the uptake to the caudate nucleus and that to the putamen. We employed the occipital cortex (OC) and total cortex (TC) as the non-specific region and calculated the ratio of specific to non-specific uptake,  $V3''(\text{OC})$  and  $V3''(\text{TC})$ , respectively, as follows. The mean values of the right and left regions were used for the calculation.

$$V3''(\text{OC}) = (\text{striate counts per voxel} - \text{OC counts per voxel}) / \text{OC counts per voxel}$$
$$V3''(\text{TC}) = (\text{striate counts per voxel} - \text{TC counts per voxel}) / \text{TC counts per voxel}$$

#### Basic and clinical evaluation

Correlation of  $V3''(\text{OC})$  or  $V3''(\text{TC})$  to  $V3''(\text{F})$ , which is considered as a standard value, was compared. Then we evaluated the possibility of differentiating PD from ET and grading the severity in these diseases.

For statistical analysis, we used the Mann-Whitney U test to compare the mean value of each  $V3''$  at a 5% level of significance. Correlation was evaluated by Pearson coefficient ( $r$ ) and Spearman rank test ( $r_s$ ).

## RESULTS

#### Basic evaluation

Correlation of  $V3''$  values calculated by fusion imaging or VOIClassic is shown in Figure 4a and 4b. A fair linear correlation was observed between  $V3''(\text{OC})$  and  $V3''(\text{F})$  ( $y = 1.53x + 1.40$ ;  $r = 0.756$ ;  $p < 0.01$ ), as well as between  $V3''(\text{TC})$  and  $V3''(\text{F})$  ( $y = 1.24x + 1.43$ ;  $r = 0.713$ ;  $p < 0.01$ ). However, the ranges of each value are different.  $V3''(\text{F})$  ranged from 0.67 to 4.17. On the other hand, both  $V3''(\text{OC})$  and  $V3''(\text{TC})$  showed higher ranges from 1.88 to 9.92 and from 1.48 to 8.39, respectively.

#### Clinical evaluation

$V3''$  values for each of the diseases were compared and are shown in Figure 5. Though  $V3''(\text{F})$  showed distinctly lower values, the distribution patterns were similar. However, one case of ET showed a  $V3''(\text{F})$  of 4.17, which was the highest value among all ET patients. On the other hand,  $V3''(\text{OC})$  and  $V3''(\text{TC})$  were 3.72 and 3.01 in this patient, which were very low.

Concerning discrimination between ET and PS, the mean  $V3''$  values are listed in the Table 1. There was a significant difference between the mean  $V3''$  of PS and ET ( $p < 0.01$ ).

Concerning the correlation between  $V3''$  value and the severity of PS, all of  $V3''(\text{F})$ ,  $V3''(\text{OC})$ , and  $V3''(\text{TC})$  values significantly correlated with the UPDRS motor score with correlation coefficient ( $r_s$ ) of  $-0.816$ ,  $-0.667$ , and  $-0.645$ , respectively (Fig. 6a, 6b, 6c).

#### Typical cases

Examples of the different striatal distribution of the tracer in two patients are shown. An ET patient (Fig. 7, Fig. 3) shows higher activity in the basal ganglia ( $V3''(\text{F})$  3.20,  $V3''(\text{OC})$  6.66,  $V3''(\text{TC})$  5.95), while a PD patient (Fig. 8a, 8b: modified Hoehn and Yahr Staging Scale of 2) shows lower ( $V3''(\text{F})$  1.18,  $V3''(\text{OC})$  3.26,  $V3''(\text{TC})$  2.93).

## DISCUSSION

Imaging of dopaminergic function is the most reliable method to differentiate patients with PD from those with other extrapyramidal diseases among all methods of diagnostic imaging. 6- $^{18}\text{F}$ fluoro-L-dopa (FDOPA) enables quantification of the deficiency of dopamine synthesis and storage inside pre-synaptic striatal nerve terminals. The rate constant ( $K_i$ ) of FDOPA for striatal uptake is thought to correlate with the striatal dopamine level, activity of dopa decarboxylase and tyrosine hydroxylase, and nigrostriatal neuron viability/density.<sup>12</sup> Investigation of striatal postsynaptic dopamine D2-receptors (D2R) is performed by SPECT using ligands such as (*S*)-2-hydroxy-3-iodo-6-methoxy-[(1-ethyl-2-pyrrolidiny)methyl]benzamide labeled with iodine-123 ( $^{123}\text{I}$ -IBZM) and (*S*)-5-iodo-7-*N*-[(1-ethyl-2-pyrrolidiny)methyl]carboxamido-2,3-dihydrobenzofuran labeled with iodine-123 ( $^{123}\text{I}$ -IBF),  $^{123}\text{I}$ -FP-CIT and 2 $\beta$ -carbomethoxy-3 $\beta$ -(4-iodophenyl)-tropane labeled with iodine-123 ( $^{123}\text{I}$ - $\beta$ -CIT) are known as agents that bind to dopamine transporters. However, the slow kinetics of  $^{123}\text{I}$ - $\beta$ -CIT is a serious drawback. A stable level of radioactivity in the striatum is reached only between 20 and 30 hr post-injection.<sup>13</sup> This indicates that optimal image acquisition can be performed only on the day following the injection of  $^{123}\text{I}$ - $\beta$ -CIT, which is highly inconvenient, especially for outpatients. Moreover, accumulated counts diminish considerably due to the short half-life of  $^{123}\text{I}$  (13.2 hr). On the other hand,  $^{123}\text{I}$ -FP-CIT allows the use of a 1-day protocol for imaging of dopamine transporters due to its fast kinetics,<sup>14,15</sup> which makes it more suitable for outpatients.

We evaluated the feasibility of VOIClassic in the semiquantitative assessment of  $^{123}\text{I}$ -FP-CIT. The result suggested that  $V3''(\text{OC})$  and  $V3''(\text{TC})$  are useful for the quantitation of  $^{123}\text{I}$ -FP-CIT uptake because of the good correlation of  $V3''(\text{OC})$  and  $V3''(\text{TC})$  with  $V3''(\text{F})$ . The cause of the difference in  $V3''$  values between VOIClassic system and fusion imaging might be due to the difference of the ROI set on the striatal accumulation. That is, VOIClassic has a three-dimensional region of caudate

nucleus and putamen to count the accumulation whereas fusion imaging utilizes only one slice. For the background, it is not essential to count the accumulation in the occipital lobe. However, in most cases the average background accumulation of total cortex (TC) was slightly higher than that of the occipital lobe (OC), which means that the accumulation average in other areas such as the frontal or temporal lobes is higher than that in the occipital lobe. The cause of this phenomenon is unknown. Anatomical normalization on Neurostat is performed by linear scaling and nonlinear warping. The average count per voxel is adjusted to be equivalent pre- and post-normalization. Then the total count might change according to variations of nonlinear warping. In this study, we estimated the  $V3''$  value with the average count per voxel. Thus inadequacy of normalization was not a problem. Another potential for cortical accumulation might depend on brain perfusion or affinity to 5HT-T.<sup>16</sup> However, the density of 5HT-T is reported to be almost the same in the frontal lobe and occipital lobe.<sup>17,18</sup> We could not clarify where to choose the non-specific region when VOIClassic is used. More investigations are needed.

The first important point for clinical evaluation concerns the capability of differentiation between ET and PS. All three parameters were useful for differentiating them. However, there was one case of ET, which showed the highest value of  $V3''(F)$  in this disease group though  $V3''(OC)$  and  $V3''(TC)$  were the lowest respectively. The SPECT image of the patient showed very clear accumulation with good background washout. However the counts of the bilateral striatal regions by the VOIClassic system were obviously much lower than those of other ET patients, and thus  $V3''(OC)$  and  $V3''(TC)$  values were low on the VOIClassic system. We pointed out that the mapping to the template was not appropriate in this case. Though the true mechanism of this misregistration is unknown, improvement of the precision of the mapping is needed.

The second point concerns the correlation between  $V3$  value and the severity of PD. There were significant negative correlations between  $V3''$  and severity expressed by the UPDRS motor score, but not by modified Hoehn and Yahr Staging Scale. It is not obvious which is the most accurate, the modified Hoehn and Yahr Staging Scale, UPDRS or  $V3''$  values, to estimate the severity of the disease. This is because the degree of the clinical severity might not strictly correlate with the true severity, i.e. the degree of neurodegeneration, due to the fact that the first symptom appears after more than 50–70% of dopaminergic function has been lost. So there is a possibility that the true severity to express the degree of the neurodegeneration might correlate better with  $V3''$  values than with the clinical severity. Various neuroprotective agents are being developed, with the intention to delay the degeneration of dopaminergic neurons. To evaluate their effectiveness, it is critical to develop methods that can reliably measure the progression of dopaminergic degeneration.<sup>19</sup>

Receptor imaging such as <sup>123</sup>I-FP-CIT is anticipated to be used for this purpose. However, further comprehensive assessment of the relevance of functional imaging to neurodegeneration or clinical severity is needed if <sup>123</sup>I-FP-CIT is to be used for assessment of disease progression, medical and surgical PD therapy strategies and possible neuroprotective applications.

## CONCLUSION

Semiquantitative analysis by VOIClassic including the Neurostat system was a useful and easy procedure for the diagnosis of early-phase PS and for differentiating it from ET. However, the correlation between  $V3''(OC)$ ,  $V3''(TC)$  value and clinical severity of PD varied. Further comprehensive assessment of the relationship between functional imaging, neurodegeneration and clinical severity is required.

## ACKNOWLEDGMENT

The authors are indebted to Prof. J. Patrick Barron of the International Medical Communications Center of Tokyo Medical University for his review of this manuscript.

## REFERENCES

1. Benamer HTS, Patterson J, Grosset DG. Accurate Differentiation of Parkinsonism and Essential Tremor Using Visual Assessment of [<sup>123</sup>I]-FP-CIT SPECT Imaging: The [<sup>123</sup>I]-FP-CIT Study Group. *Movement Disorders* 2000; 15: 503–510.
2. Booji J, Sokole EB, Stabin MG, Janssen AGM, Bruin K, Van Royen EA. Human biodistribution and dosimetry of [<sup>123</sup>I]FP-CIT: a potent radioligand for imaging of dopamine transporters. *Eur J Nucl Med* 1998; 25: 24–30.
3. Booji J, Tissingh G, Boer GJ, Speelman JD, Stoof JC, Janssen AGM, et al. [<sup>123</sup>I]FP-CIT SPECT shows a pronounced decline of striatal dopamine transporter labeling in early and advanced Parkinson's disease. *J Neurol Neurosurg Psychiatry* 1997; 62: 133–140.
4. Colloby SJ, O'Brien JT, Fenwick JD, Firbank MJ, Burn DJ, McKeith IG, et al. The application of statistical parametric mapping to [<sup>123</sup>I]FP-CIT SPECT in dementia with Lewy bodies, Alzheimer's disease and Parkinson's disease. *Neuroimage* 2004; 23: 956–966.
5. Larucelle M, Wallace E, Seibyl JP, Baldwin RM, Zea-Pnoce Y, Zoghbi SS, et al. Graphical, kinetic, and equilibrium analyses of *in vivo* [<sup>123</sup>I]β-CIT binding to dopamine transporters in healthy human subjects. *J Cereb Blood Flow Metab* 1994; 14: 982–994.
6. Kuikka JT, Bergström KA, Vanninen E, Laulumaa V, Hartikainen P, Lämsimies E, et al. Initial experience with single-photon emission tomography using iodine-123-labelled 2β-carbomethoxy-3β-(4-iodophenyl)tropane in human brain. *Eur J Nucl Med* 1993; 20: 783–786.
7. Tsuchida T, Ballinger JR, Vines D, Kim YJ, Utsunomiya K, Lang AE, et al. Reproducibility of dopamine transporter density measured with <sup>123</sup>I-FPCIT SPECT in normal

- control and Parkinson's disease patients. *Ann Nucl Med* 2004; 18: 609–616.
8. Lucignani G, Gobbo C, Moresco RM, Antoni A, Panzacchi A, Bonaldi L, et al. The feasibility of statistical parametric mapping for the analysis of positron emission tomography studies using  $^{11}\text{C}$ -2- $\beta$ -carbomethoxy-3- $\beta$ -(4-fluorophenyl)-tropane in patients with movement disorders. *Nucl Med Commun* 2002; 23: 1047–1055.
  9. Messa C, Volonté MA, Fazio F, Zito F, Carpinelli A, d'Amico A, et al. Differential distribution of striatal [ $^{123}\text{I}$ ] $\beta$ -CIT in Parkinson's disease and progressive supranuclear palsy, evaluated with single-photon emission tomography. *Eur J Nucl Med* 1998; 25: 1270–1276.
  10. Minoshima S, Koeppe RA, Frey KA, Kuhl DE. Anatomic standardization: linear scaling and nonlinear warping of functional brain images. *J Nucl Med* 1994; 35: 1528–1537.
  11. Hosaka K, Ishii K, Sakamoto S, Sadato N, Fukuda H, Kato T, et al. Validation of anatomical standardization of FDG PET images of normal brain: comparison of SPM and NEUROSTAT. *Eur J Nucl Med Mol Imaging* 2005; 32: 92–97.
  12. Antonini A, Leenders KL, Vontobel P, Maguire P, Missimer J, Psylla M, et al. Complementary PET studies of striatal neuronal function in the differential diagnosis between multiple system atrophy and Parkinson's disease. *Brain* 1997; 120: 2187–2195.
  13. Seibyl JP, Laruelle M, van Dyck CH, Wallace E, Baldwin RM, Zoghbi S, et al. Reproducibility of Iodine-123- $\beta$ -CIT SPECT brain measurement of dopamine transporters. *J Nucl Med* 1996; 37: 222–228.
  14. Booji J, Hemelaar JTGM, Spleeman JD, Bruin K, Janssen AGM, Van Royen EA, et al. One-day Protocol for Imaging of the Nigrostriatal Dopaminergic Pathway in Parkinson's Disease by [ $^{123}\text{I}$ ]FP-CIT SPECT. *J Nucl Med* 1999; 40: 753–761.
  15. Kuikka JT, Bergström KA, Ahonen A, Hiltunen J, Haukka J, Lansimies E, et al. Comparison of iodine-123 labelled 2 $\beta$ -carbomethoxy-3 $\beta$ -(4-iodophenyl)tropane and 2 $\beta$ -carbomethoxy-3 $\beta$ -(4-iodophenyl)-*N*-(3-fluoropropyl)nortropane for imaging of the dopamine transporter in the living human brain. *Eur J Nucl Med* 1995; 22: 356–360.
  16. Takano K, Matsumura K, Watanabe Y, Yamada T, Kubo H, Naitou Y, et al. Phase I clinical study of  $^{123}\text{I}$ -FP-CIT, a new radioligand for evaluating dopamine transporter by SPECT (II): Tracer kinetics in brain. *KAKU IGAKU (Jpn J Nucl Med)* 1999; 36: 1013–1022.
  17. Bäckström I, Bergström M, Marcusson J. High affinity [ $^3\text{H}$ ] paroxetine binding to serotonin uptake sites in human brain tissue. *Brain Res* 1989; 486: 261–286.
  18. Chinaglia G, Landwehrmeyer B, Probst A, Palacios JM. Serotonergic terminal transporters are differentially affected in Parkinson's disease and progressive supranuclear palsy: an autoradiographic study with [ $^3\text{H}$ ]citalopram. *Neuroscience* 1993; 54: 691–699.
  19. Schapira AHV, Olanow CW. Neuroprotection in Parkinson disease—Mysteries, Myths, and Misconceptions. *JAMA* 2004; 291: 358–364.